Inclusive $^{12}C(\nu_\mu,\mu)^{12}N$ reaction in the continuum random phase approximation

E. Kolbe,[1] K. Langanke,[2] F.-K. Thielemann,[1] and P. Vogel[3]
[1]*Physikalisches Institut, Universität Basel, Basel, Switzerland*
[2]*W. K. Kellogg Radiation Laboratory, 106-38, California Institute of Technology, Pasadena, California 91125*
[3]*Physics Department, California Institute of Technology, Pasadena, California 91125*
(Received 21 July 1995)

Motivated by a recent experiment at LAMPF we calculate cross sections for muon-neutrino and muon-antineutrino charged-current reactions on ^{12}C within the continuum RPA model. We also determine the branching ratios for the main decay channels of these reactions by application of a statistical model.

PACS number(s): 25.30.Pt, 21.60.Jz, 23.40.Bw, 27.20.+n

In recent years accelerator-based studies of neutrino-induced reactions have become feasible. In particular, the charged-current reactions on ^{12}C, induced by both electron- [1] and muon-neutrinos [2,3] have been measured exciting the ^{12}N ground state and the continuum states in ^{12}N. The exclusive $^{12}C(\nu_e,e)^{12}N_{g.s.}$ cross section measured by the KARMEN Collaboration is consistent with other data (β-decay, muon capture) which depend on the unique weak nuclear matrix element connecting the ^{12}C ground state with the ^{12}N and ^{12}B mirror ground states [1,4]. Theoretical predictions for this exclusive cross section are in good agreement with the data [4–6]. The very recent measurement of the $^{12}C(\nu_\mu,\mu)^{12}N_{g.s.}$ reaction, although still with large error bars, is consistent with the other measurements [3,7]. We note that a previously reported measurement of the same exclusive cross section [2] appears to be inconsistently large [3,4]; we will not further discuss that measurement here.

The KARMEN Collaboration also determined the inclusive $^{12}C(\nu_e,e)^{12}N^*$ cross section leading to various continuum states in ^{12}N. The same cross section has been measured at LAMPF, however with large errors [8]. These experiments, and the study of the muon capture $^{12}C(\mu,\nu_\mu)^{12}B^*$ to the continuum states in ^{12}B, which is the mirror nucleus of ^{12}N, are related. In fact, the $^{12}C(\nu_e,e)^{12}N^*$ cross section and the total $^{12}C(\mu,\nu_\mu)^{12}B^*$ muon capture rate appear to be consistent and both are well reproduced (within a few percent) by a continuum random phase calculation [4,9]. Noticeably, the results presented in Ref. [9] are independent of the adopted residual interaction.

In addition to the existing $^{12}C(\nu_e,e)^{12}N^*$ and $^{12}C(\mu,\nu_\mu)^{12}B^*$ data, the LSND Collaboration has very recently reported a measurement of the $^{12}C(\nu_\mu,\mu)^{12}N^*$ cross section using the LAMPF pion decay-in-flight ν_μ-neutrino beam. Here we describe detailed evaluations of the $^{12}C(\nu_\mu,\mu)^{12}N^*$ reaction. The calculations have been performed within the same framework of the continuum random phase approximation which has been applied to the $^{12}C(\nu_e,e)^{12}N^*$ and $^{12}C(\mu,\nu_\mu)^{12}B^*$ reactions earlier [4,9]. The model is described in details in Refs. [10,11]. As residual interaction we adopt the finite-range force based on the Bonn potential [12]; calculations employing the zero-range Landau-Migdal force [11] give very similar results. We like to point out that our calculation is parameter-free in the sense that no parameter has been adjusted to any weak-interaction data. For the axial vector coupling constant we use the free-nucleon value $g_A=1.25$; for a discussion of this choice see [9]. The Coulomb interaction between the muon and the residual nucleus has been taken into account.

The final states in ^{12}N are expected to decay mainly by proton emission. The LSND cannot distinguish between the muon and proton energies (E_p and E_μ, respectively), but rather measures only the total deposited energy, $E_{det}=\alpha E_\mu+\beta E_p$ with particle-energy dependent detector efficiencies α,β. While the muon spectrum is obtained in our model naturally when calculating the differential cross section as function of the excitation energy [4], the calculation of the proton spectrum needs some extra care. First, the final ^{12}N states, if above the appropriate thresholds, can decay into different channels. Second, these decays can go to excited levels in the residual nucleus rather than to its ground state. The consideration of such cascade transitions is quite important for the proton spectrum, as it will shift the spectrum to lower proton energies. Our calculation of the cascade is based on the statistical model using the well-established model code SMOKER [13]. [A similar approach has been used to calculate the $(\nu,\nu'p)$ and $(\nu,\nu'n)$ cross sections on ^{12}C and has been tested against the integrated photodissociation data on this nucleus [11].]

In the first step we have calculated the $^{12}C(\nu_\mu,\mu)^{12}N^*$ cross section as a function of excitation energy in ^{12}N within the continuum random phase approximation. For each final state, with well-defined energy, angular momentum, and parity, we have calculated the branching ratios into the various decay channels, considering proton, neutron, α and γ emission. As possible final states in the residual nucleus the SMOKER code considers the experimentally known levels supplemented at higher energies by an appropriate level density formula [13]. If the decay leads to an excited level of the residual nucleus (e.g., to $p+^{11}C^*$), we have calculated the branching ratios for the decay of this level in an analogous way. Keeping track of the energies of the ejected particles and photons during the cascade and, weighting them with appropriate branching ratios and the corresponding differential $^{12}C(\nu_\mu,\mu)^{12}N^*$ cross section, we determined the various particle (proton, neutron, α) and photon spectra for the (ν_μ,μ^-) reaction on ^{12}C. We have performed a similar calculation for the $(\bar{\nu}_\mu,\mu^+)$ reaction on ^{12}C leading to intermediate states in ^{12}B. For both reactions our results have

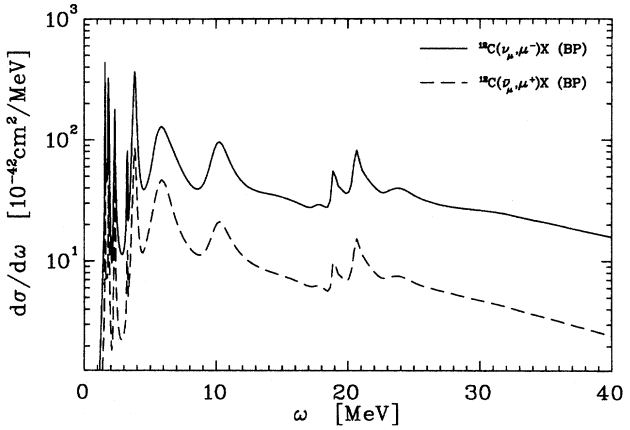

FIG. 1. The $^{12}C(\nu_\mu,\mu^-)^{12}N$ and $^{12}C(\bar{\nu}_\mu,\mu^+)^{12}B$ cross sections as function of excitation energy.

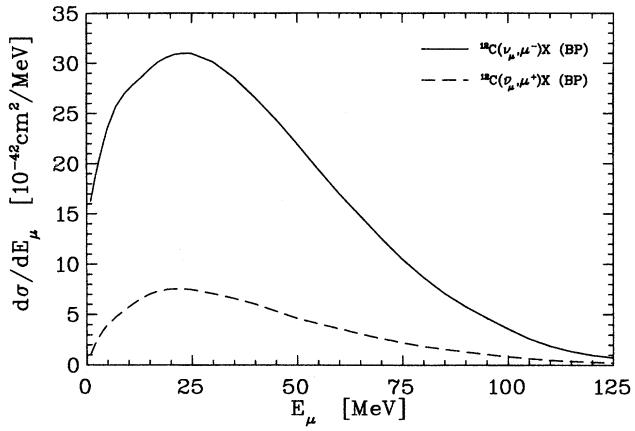

FIG. 2. The muon distribution for the inclusive $^{12}C(\nu_\mu,\mu^-)^{12}N^*$ and $^{12}C(\bar{\nu}_\mu,\mu^+)^{12}B$ reactions.

been averaged over the appropriate LSND neutrino distributions for neutrino energies from threshold to 280 MeV.

Our flux-averaged total $^{12}C(\nu_\mu,\mu)^{12}N^*$ cross section is 19.3×10^{-40} cm^2 (using the Migdal interaction [11] we calculate a total cross section of 20.3×10^{-40} cm^2), including a contribution of 0.63×10^{-40} cm^2 for the transition to the ^{12}N ground state. While the latter appears to be in agreement with the LSND observation [3,7], our calculated total cross section is more than twice the reported experimental value, $\sigma_{expt}=(8.3\pm0.7\pm1.6)\times10^{-40}$ cm^2 [3]. The calculated cross section is shown as a function of excitation energy in Fig. 1. For the inclusive $^{12}C(\bar{\nu}_\mu,\mu^+)^{12}B^*$ cross section we calculate 4.2×10^{-40} cm^2.

One can think of several effects that lower the calculated cross sections. For example, the quenching of the axial vector coupling constant [14] or a reduced value of the effective nucleon mass in the nuclear medium due to relativistic effects [15] both decrease the $^{12}C(\nu_\mu,\mu^-)^{12}N^*$ cross section. However, similar corrections apply to the muon capture, and to a lesser extent, to the $^{12}C(\nu_e,e^-)^{12}N^*$ reaction. Reference [9] has shown that using the "quenched value" $g_A=1$ for the axial vector coupling constant lowers the muon-capture rate by about 30% destroying the good agreement between the (present) continuum RPA formalism and the data. Kim *et al.* [15] have noted that the relativistic medium modification of the effective nucleon mass reduces the $^{12}C(\nu_\mu,\mu^-)^{12}N^*$ cross section by about 30%, which by itself is not enough to bring the present random phase results into agreement with the data. Moreover, the same correction are expected to lower the $^{12}C(\nu_e,e^-)^{12}N^*$ cross section by about 20% [15] in which case the present formalism barely agrees with the KARMEN data at their lower limit. Presumably the muon capture rate would also be lowered, thus destroying the nice reproduction of the data obtained in [9]. Medium modifications of the momentum transfer dependence of the nuclear form factors will not affect the calculations as the momentum transfer is too small in all three experiments. Thus neither of the discussed potential corrections allows a consistent description of the three processes [$^{12}C(\nu_e,e^-)^{12}N^*$, $^{12}C(\nu_\mu,\mu^-)^{12}N^*$, and $^{12}C(\mu,\nu_\mu)^{12}B^*$] within the current model.

The RPA includes 1p-1h (one-particle–one-hole) correlations which are responsible for most of the nuclear response under consideration. However, the corresponding strength is also spread and partially shifted upward by the 2p-2h [16] and other multiparticle-multihole correlations, reducing the cross section somewhat. This reduction should be more pronounced, however, in the ν_e induced reaction and in the muon capture, where low-lying strength is more important, than in the ν_μ induced reaction where higher-lying strength is important. Thus, we believe, the inclusion of 2p-2h correlations would make the inconsistency between the ν_e induced reaction and the muon capture on one hand, and the ν_μ induced reaction on the other hand, even worse.

Naively, the $^{12}C(\nu_\mu,\mu^-)^{12}N^*$ reaction, as measured with the LAMPF neutrino beam, and the $^{12}C(\mu,\nu_\mu)^{12}B^*$ muon capture process might be viewed as "inverse reactions," taking into account that ^{12}B and ^{12}N are mirror nuclei. However, the muon capture process is dominated by the capture to the giant resonances with $J^\pi=1^-$ and 2^-. These two multipolarities account for more than 80% of the total rate for transitions leading to continuum states. On the other hand, for the $^{12}C(\nu_\mu,\mu^-)^{12}N^*$ reaction these multipoles contribute only about 50% of the cross section. In other words, the strength distributions in these two reactions are not identical, with muon capture populating typically lower-lying states than the (ν_μ,μ^-) reaction for the LAMPF ν_μ spectrum. Note that the energy positions of the 1^- and 2^- resonances, as calculated in the present approach, agree well with experiment [11].

Figure 2 shows the muon spectrum for the inclusive $^{12}C(\nu_\mu,\mu)^{12}N^*$ reaction. The spectrum is centered around a kinetic energy of 23 MeV with a width of about 25 MeV. We find that, even for a fixed neutrino energy, many nuclear states contribute to the inclusive cross section, invalidating the use of the so-called elementary particle approach for the inclusive reaction. The accuracy of the results obtained in Ref. [17] for the $^{12}C(\nu_\mu,\mu^-)^{12}N^*$ cross section using the elementary particle model is therefore questionable, as already noted by Kubodera and Nozawa [18].

Following the decay cascade in the residual nuclei, we calculated the various particle and photon spectra. These results might be helpful in future experiments to pin down the origin of the discrepancy between our calculation and data

TABLE I. Total and partial cross sections and braching ratios. The lower part shows the branches following the main decay of the initially excited nucleus.

Reaction	$\sigma_{tot}[10^{-42}$ cm$^2]$	%	Reaction	$\sigma_{tot}[10^{-42}$ cm$^2]$	%
$^{12}C(\nu_\mu,\mu^-)X$	1925	100.0	$^{12}C(\bar{\nu}_\mu,\mu^+)X$	423	100.0
$^{12}C(\nu_\mu,\mu^-)^{12}N_{g.s.}$	63	3.3	$^{12}C(\bar{\nu}_\mu,\mu^+)^{12}B_{g.s.}$	26	6.1
$^{12}C(\nu_\mu,\mu^- p)^{11}C$	1627	84.5	$^{12}C(\bar{\nu}_\mu,\mu^+ p)^{11}Be$	19	4.5
$^{12}C(\nu_\mu,\mu^- n)^{11}N$	89	4.6	$^{12}C(\bar{\nu}_\mu,\mu^+ n)^{11}B$	333	78.8
$^{12}C(\nu_\mu,\mu^-\alpha)^{8}B$	145	7.5	$^{12}C(\bar{\nu}_\mu,\mu^+\alpha)^{8}Li$	32	7.5
$^{12}C(\nu_\mu,\mu^-\gamma)^{12}N$	0	0.0	$^{12}C(\bar{\nu}_\mu,\mu^+\gamma)^{12}B$	13	3.2
TOTAL	1925	100.0	TOTAL	423	100.0
$^{12}C(\nu_\mu,\mu^- p)^{11}C_{g.s.}$	529	27.5	$^{12}C(\bar{\nu}_\mu,\mu^+ n)^{11}B_{g.s.}$	142	33.6
$^{12}C(\nu_\mu,\mu^- p\gamma)^{11}C_{g.s.}$	390	20.3	$^{12}C(\bar{\nu}_\mu,\mu^+ n\gamma)^{11}B_{g.s.}$	93	22.0
$^{12}C(\nu_\mu,\mu^- pn)^{10}C$	24	1.3	$^{12}C(\bar{\nu}_\mu,\mu^+ np)^{10}C$	12	2.8
$^{12}C(\nu_\mu,\mu^- 2p)^{10}B$	333	17.3	$^{12}C(\bar{\nu}_\mu,\mu^+ 2n)^{10}B$	33	7.8
$^{12}C(\nu_\mu,\mu^- p\alpha)^{7}Be$	351	18.2	$^{12}C(\bar{\nu}_\mu,\mu^+ n\alpha)^{7}Li$	54	12.7
TOTAL	1627	84.5	TOTAL	333	78.8

for the inclusive $^{12}C(\nu_\mu,\mu)^{12}N^*$ reaction. Table I lists the branchings of the final ^{12}N (and ^{12}B) states into the various decay channels, integrated over all excitation energies in ^{12}N and weighted by the $^{12}C(\nu_\mu,\mu)^{12}N^*$ cross section. As expected, the dominating decay mode is proton emission (84.5%), but we calculate also a neutron-decay branch ($\approx$5%), which stems mainly from the decay at very high excitation energies where in our statistical model the dominance of the proton decay over neutron decay due to the difference in the threshold values becomes less important. We find that only in 27.5% of all cases the proton decay is to the ^{11}C ground state.

Table I also lists the branchings, integrated over the final states in the residual ^{11}C (and ^{11}B) nucleus. In roughly 20% of the cases ^{11}C is populated in a state below particle thresholds and thus decays by γ emission. These γ decays will also contribute to the light yield observed in the LSND. If ^{11}C is in an excited state above particle thresholds, it decays by α and proton emission, where the first channel is favored by the lower Q value. In a rare 1% of all cases, the proton decay of ^{12}N is followed by a neutron decay of an excited level in ^{11}C. We thus find that in about 6% of all events, the $^{12}C(\nu_\mu,\mu)^{12}N^*$ reaction generates a neutron in the final channel. It would be important to verify this branching ratio experimentally. However, for the LSND this is not easy, since for this detector most of the (μ,n) pairs arise from the $\bar{\nu}_\mu$ reaction on protons, as discussed below.

As the majority of decays of the $^{12}N^*$ levels, populated by the $^{12}C(\nu_\mu,\mu^-)^{12}N^*$ reaction, is to excited levels in ^{11}C (which might be followed by the emission of a second proton in the subsequent ^{11}C decay), the cascade transitions shift the proton spectrum in the inclusive $^{12}C(\nu_\mu,\mu^-)^{12}N^*$ reaction clearly to lower energies compared to a spectrum for proton decay to the ^{11}C ground state. This is demonstrated in Fig. 3. The proton spectrum is centered at rather low energies and protons with energies larger than 15 MeV are rare. This finding might justify replacing the proton spectrum approximately by the average energy $\bar{E}_p \approx 9$ MeV. Note that this value is significantly smaller than the mean excitation energy $\bar{\omega} \approx 20$ MeV which corresponds to the average proton energy (except for a shift of 0.6 MeV reflecting the proton threshold in ^{12}N) if the decay of the $^{12}N^*$ states were to the ^{11}C ground state only.

Figure 3 also shows the γ spectrum of the cascade. As the photons originate from decays of ^{11}C levels below the particle thresholds, the respective γ energies are necessarily smaller than 7.5 MeV. As in the case of the proton spectrum, the γ spectrum might be replaced approximately by the average energy $\bar{E}_\gamma \approx 4.0$ MeV. Thus, the observed "muon +proton" spectrum in Ref. [3] should correspond approximately to the muon spectrum, distorted by the coefficient α and shifted by the energy $\beta\bar{E}_p + \delta\bar{E}_\gamma \approx 3.8$ MeV, where we have used $\beta = 0.4$ (this value does not include the branching ratio of 0.845) and the coefficient $\delta = 0.2$ accounts for the fact that photons are observed only in about 20% of all (ν_μ,μ^-) events. In fact, if we adopt a reasonable value of $\alpha = 0.6$ and apply a constant energy shift of 3.8 MeV to account for the combined proton and γ contributions, the measured spectrum as reported in Ref. [3] agrees well with our calculated muon spectrum at all energies. As scaling factor we adopted 25.6 photoelectrons per MeV from [3]. Figure 4 shows the neutron and γ spectrum for the $^{12}C(\bar{\nu}_\mu,\mu^+)^{12}B^*$ reaction.

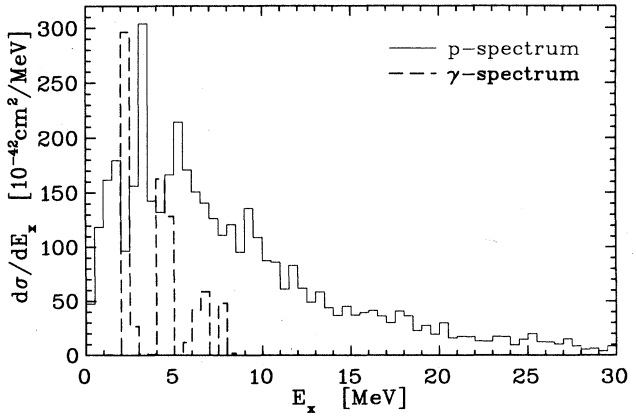

FIG. 3. The proton and γ spectra for the $^{12}C(\nu_\mu,\mu^-)$ reaction.

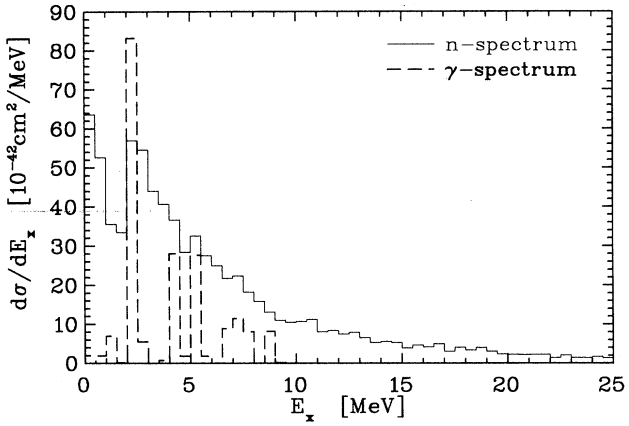

FIG. 4. The neutron and γ spectra for the $^{12}C(\bar{\nu}_\mu,\mu^+)$ reaction.

The delayed coincidence detection of a positron and a neutron (identified by the 2.23 MeV γ ray emitted after the neutron capture on a free proton) constitutes the signal for $\bar{\nu}_\mu \rightarrow \bar{\nu}_e$ appearance oscillations in the LSND [19]. Important backgrounds are assumed to stem from small $\bar{\nu}_e$ and $\bar{\nu}_\mu$ admixtures in the neutrino beam which via the charged-current reaction on free protons in the scintillator might mimic the signal (lepton+neutron). We have calculated the $\bar{\nu}_e + p \rightarrow n + e^+$ cross section as 0.9×10^{-40} cm^2, where we assumed that the $\bar{\nu}_e$ originate from the μ^- decay at rest. If we take instead the spectrum of $\bar{\nu}_\mu$ from the μ^+ decay at rest, and assume the complete conversion $\bar{\nu}_\mu \rightarrow \bar{\nu}_e$, the same cross section increases to 1.1×10^{-40} cm^2, because the $\bar{\nu}_e$ have now higher average energy.

The "decay in flight" neutrino beam contains $\bar{\nu}_\mu$ neutrinos, originating from the π^- decay in flight. The corresponding cross section for the reaction $\bar{\nu}_\mu + p \rightarrow n + \mu^+$ is 4.0×10^{-40} cm^2, where we have normalized the spectrum to the unit $\bar{\nu}_\mu$ flux above the threshold for the reaction on free protons ($E_{\bar{\nu}} = 112.4$ MeV). Again, if one were to assume that all of these $\bar{\nu}_\mu$ oscillate into $\bar{\nu}_e$, the reaction cross section on free protons increases to 1.7×10^{-39} cm^2, for the same flux normalization.

As we have discussed above, neutrons and leptons are also generated in the ν_μ and $\bar{\nu}_\mu$ induced charged-current reactions on ^{12}C, where the positrons and electrons will be produced in the respective muon decays. These events will represent backgrounds in the $\bar{\nu}_\mu \rightarrow \bar{\nu}_e$ oscillation search if the muon is lost or is misidentified as an electron [19]. From Table I we find the total $^{12}C(\bar{\nu}_\mu,\mu^+n)^{11}B$ cross section to be about 3.3×10^{-40} cm^2. If we consider that there are about twice as many free protons in the detector than ^{12}C nuclei, the $^{12}C(\bar{\nu}_\mu,\mu^+n)^{11}B$ reaction is likely to produce roughly a 40% of the background signals expected from the $\bar{\nu}_\mu$ reaction on free protons. Our calculation gives the $^{12}C(\nu_\mu,\mu^-n)^{11}N$ cross section as 0.9×10^{-40} cm^2. Considering that the intensity of the ν_μ beam is about seven times larger than the one of the $\bar{\nu}_\mu$ beam, we expect therefore about twice as many background signals from this reaction

TABLE II. Total $^{12}C(\nu_e,e^-)^{12}N$ and $^{12}C(\bar{\nu}_e,e^+)^{12}B$ cross sections and partial cross sections to the ^{12}N and ^{12}B ground states for selected neutrino energies E_ν. The cross sections are given in 10^{-42} cm^2, while the energies are in MeV. Exponents are given in parentheses.

E_ν	$^{12}C(\nu_e,e^-)^{12}N$	$^{12}C(\nu_e,e^-)^{12}N_{g.s.}$	$^{12}C(\bar{\nu}_e,e^+)^{12}B$	$^{12}C(\bar{\nu}_e,e^+)^{12}B_{g.s.}$
20	3.14(−1)	3.13(−1)	8.02(−1)	7.90(−1)
30	6.29	5.34	6.27	4.98
40	2.54(+1)	1.57(+1)	1.98(+1)	1.15(+1)
50	6.89(+1)	2.98(+1)	4.55(+1)	1.90(+1)
60	1.51(+2)	4.53(+1)	8.68(+1)	2.62(+1)
70	2.85(+2)	6.00(+1)	1.45(+2)	3.24(+1)
80	4.81(+2)	7.26(+1)	2.22(+2)	3.72(+1)
90	7.49(+2)	8.21(+1)	3.15(+2)	4.07(+1)
100	1.09(+3)	8.83(+1)	4.23(+2)	4.31(+1)
110	1.51(+3)	9.15(+1)	5.45(+2)	4.47(+1)
120	2.02(+3)	9.23(+1)	6.80(+2)	4.57(+1)
130	2.60(+3)	9.15(+1)	8.26(+2)	4.65(+1)
140	3.28(+3)	8.97(+1)	9.82(+2)	4.71(+1)
150	4.04(+3)	8.75(+1)	1.15(+3)	4.77(+1)
160	4.90(+3)	8.55(+1)	1.32(+3)	4.82(+1)
170	5.84(+3)	8.38(+1)	1.51(+3)	4.87(+1)
180	6.87(+3)	8.24(+1)	1.69(+3)	4.92(+1)
190	7.98(+3)	8.13(+1)	1.88(+3)	4.97(+1)
200	9.15(+3)	8.05(+1)	2.08(+3)	5.01(+1)
210	1.04(+4)	7.98(+1)	2.27(+3)	5.06(+1)
220	1.17(+4)	7.92(+1)	2.47(+3)	5.10(+1)
230	1.30(+4)	7.87(+1)	2.67(+3)	5.14(+1)
240	1.44(+4)	7.82(+1)	2.87(+3)	5.18(+1)
250	1.57(+4)	7.77(+1)	3.07(+3)	5.22(+1)

than from the $^{12}C(\bar{\nu}_\mu,\mu^+n)^{11}B$ reaction. However, in absolute terms the neutrino reactions on ^{12}C are only a small part of the total background expected in the LSND neutrino oscillation experiment (see Table II in [19]). From our cross-section estimates we expect the background to rise by less than 20% if the neutrino reactions on ^{12}C are included. (This estimate could be further reduced if our calculated neutron-producing cross sections are too large, similarly to the total reaction cross sections, as discussed above.)

The LSND Collaboration indeed observes certain number of muon+neutron events [20]. When all these events are assumed to originate in the $\bar{\nu}_\mu+p\rightarrow n+\mu^+$ reaction, the flux averaged cross section of $4.1\pm1.0(\text{stat})\pm0.5(\text{syst})\times10^{-40}$ cm^2 is deduced [20], in agreement with our calculation above. However, we argued above that only about half of the expected muon+neutron *events* originates in the $\bar{\nu}_\mu+p\rightarrow n+\mu^+$ reaction, while the other half stems from the $^{12}C(\bar{\nu}_\mu,\mu^+n)^{11}B^*$ and $^{12}C(\nu_\mu,\mu^-n)^{11}N^*$ reactions. Thus, again we see that even for the exclusive channel of the muon +neutron events, the calculation predicts approximately twice as many events than actually observed.

In the LAMPF neutrino beam ν_e neutrinos with energies larger than the end point of the Michel spectrum, $E_\nu>53$ MeV, are virtually absent. However, high-energy ν_e neutrinos can be generated by possible $\nu_\mu\rightarrow\nu_e$ oscillations. Thus, the observation of charged-current reactions induced by high-energy electron neutrinos offer a complementary signal for the presence of neutrino oscillations in the LSND. To assist the analysis of the experiment in the search for these events, we have calculated the relevant $^{12}C(\nu_e,e^-)^{12}B$ cross sections within the same continuum random phase approximation as adopted above. Since the $\nu_\mu\rightarrow\nu_e$ oscillation probability is in general a function of neutrino energy, we prefer to present the relevant cross sections as a function of incident neutrino energy. The results are listed in Table II which also gives the cross sections for the $\bar{\nu}_e$-induced charged-current reaction on ^{12}C. Observation of the high-energy electrons would be an important confirmation of the oscillation hypothesis. The yield, however, would depend not only on the neutrino oscillation parameters, but also on the cross sections in Table II.

In conclusion, we presented results of our analysis of the interaction of muon neutrinos (and antineutrinos) with ^{12}C. We stressed that the discrepancy with the LSND measurements [3] is not understood, and contrasted it with the good agreement between experiments and calculations for the (ν_e,e^-) and muon capture reactions on ^{12}C. These latter two reactions populate the same states in the final nucleus ^{12}N (and its mirror ^{12}B), but the average excitation energy is somewhat less than for the LSND experiment.

To facilitate the search for the origin of this puzzling discrepancy, we also calculated the spectra and branching ratios of the decay of the final nuclei. In particular, we predict a potentially observable $\approx6\%$ neutron branch for the (ν_μ,μ^-) reaction on ^{12}C at LSND. The importance of resolving this puzzle in the emerging field of low-energy neutrino-nucleus interaction is obvious.

We thank R.L. Burman, W.C. Louis, and R.D. McKeown for helpful discussions. This work was supported by the U.S. National Science Foundation (Grants Nos. PHY91-15574, PHY94-12818, and PHY94-20470), by the U.S. Department of Energy (DE-FG03-88ER-40397), and by the Swiss Nationalfonds.

[1] KARMEN Collaboration, G. Drexlin *et al.*, in *Proceedings of Neutrino Workshop-Heidelberg 1987*, edited by B. Povh and V. Klapdor (Springer-Verlag, Berlin, 1988), p. 147; KARMEN Collaboration, G. Drexlin *et al.*, Phys. Lett. B **267**, 321 (1991); KARMEN Collaboration, B. Zeitnitz, Prog. Part. Nucl. Phys. **32**, 351 (1994).
[2] D.D. Koetke *et al.*, Phys. Rev. C **46**, 2554 (1992).
[3] M. Albert *et al.*, Phys. Rev. C **51**, 1065 (1995).
[4] E. Kolbe, K. Langanke, and S. Krewald, Phys. Rev. C **49**, 1122 (1994).
[5] T.W. Donnelly, Phys. Lett. **43B**, 93 (1973).
[6] M. Fukugita, Y. Kohyama, and K. Kubodera, Phys. Lett. B **212**, 139 (1988).
[7] W.C. Louis (private communication).
[8] D.A. Krakauer *et al.*, Phys. Rev. C **45**, 2450 (1992).
[9] E. Kolbe, K. Langanke, and P. Vogel, Phys. Rev. C **50**, 2576 (1994).
[10] M. Buballa, S. Drożdż, S. Krewald, and J. Speth, Ann. Phys. (N.Y.) **208**, 346 (1991).
[11] E. Kolbe, K. Langanke, S. Krewald, and F.-K. Thielemann, Nucl. Phys. **A540**, 599 (1992).
[12] K. Nakayama, S. Drożdż, S. Krewald, and J. Speth, Nucl. Phys. **A470**, 573 (1987).
[13] J.J. Cowan, F.-K. Thielemann, and J.W. Truran, Phys. Rep. **208**, 267 (1991).
[14] B.A. Brown and B.H. Wildenthal, Annu. Rev. Nucl. Part. Sci. **38**, 29 (1988).
[15] H. Kim, J. Piekarewicz, and C.J. Horowitz, Florida State University Report No. FSU-SCRI-95-20, 1995 (unpublished).
[16] S. Drozdz, S. Nishizaki, J. Speth, and J. Wambach, Phys. Rep. **197**, 1 (1990).
[17] C.W. Kim and S.L. Mintz, Phys. Rev. C **31**, 274 (1985).
[18] K. Kubodera and S. Nozawa, Int. J. Mod. Phys. **3**, 101 (1994).
[19] C. Athanassopoulos *et al.*, Phys. Rev. Lett. **75**, 2650 (1995).
[20] C. Athanassopoulos, Ph.D. thesis, Temple University, 1995.